Development and mechanical properties of a locking T-plate[1]

Luciane R. Mesquita[2], Sheila C. Rahal[2]*, Camilo Mesquita Neto[3], Washington T. Kano[2], Antônio C. Beato[3], Luís G. Faria[2] and Maíra S. Castilho[2]

ABSTRACT.- Mesquita L.R., Rahal S.C., Mesquita Neto C., Kano W.T., Beato A.C., Faria L.G. & Castilho M.S. 2017. **Development and mechanical properties of a locking T-plate.** *Pesquisa Veterinária Brasileira 37(5):495-501*. Department of Veterinary Surgery and Anesthesiology, School of Veterinary Medicine and Animal Science, Universidade Estadual Paulista, Cx. Postal 560, Rubião Júnior s/n, Botucatu, SP 18618-000, Brazil. E-mail: sheilacr@fmvz.unesp.br

This study aimed to develop a locking T-plate and to evaluate its mechanical properties in synthetic models. A titanium 2.7mm T-plate was designed with a shaft containing three locked screw holes and one dynamic compression hole, and a head with two locked screw holes. Forty T-shaped polyurethane blocks, and 20 T-plates were used for mechanical testing. Six bone-plate constructs were tested to failure, three in axial compression and three in cantilever bending. Fourteen bone-plate constructs were tested for failure in fatigue, seven in axial compression and seven in cantilever bending. In static testing *higher values of axial compression test than cantilever bending test were observed for all variables.* In axial compression fatigue testing all bone-plate constructs withstood 1,000,000 cycles. Four bone-plate constructs failure occurred before 1,000,000 cycles in cantilever bending fatigue testing. In conclusion, *the* locking T-plate tested has mechanical properties that offer greatest resistance to fracture under axial loading than bending forces.

INDEX TERMS: Bone-plate, implant, fracture, mechanical study.

RESUMO.- [**Desenvolvimento e as propriedades mecânicas de uma placa bloqueada em formato de T.**] O objetivo deste estudo foi desenvolver uma placa bloqueada em formato de T e avaliar as propriedades mecânicas em um modelo sintético. Uma placa-T em liga de titânio 2,7mm foi desenhada com uma haste contendo três orifícios para parafusos bloqueados e um orifício para realização de compressão dinâmica. 40 blocos de poliuretano em formato de T e 20 placas-T foram utilizados para os ensaios mecânicos. Seis montagens osso-placa foram testados até a falha, sendo três em força de compressão axial e três em flexão engastada. 14 montagens osso-placa foram testadas até a falha em fatiga, sendo 7 em força de compressão axial e 7 em flexão engastada. No teste estático, os valores mais altos foram observados em todas as variáveis no teste de compressão axial quando comparado à flexão engastada. Já nos testes de fadiga na força de compressão axial, todas as montagens osso-placa resistiram à 1000000 de ciclos. No teste de fadiga em flexão engastada, quatro montagens osso-placa falharam antes de alcançarem 1000000 de ciclos. Em conclusão, a placa-T estudada apresenta propriedades mecânicas que oferecem uma melhor resistência em estabilizar as fraturas na atuação das forças de compressão axial que nas forças de flexão.

TERMOS DE IDEXAÇÃO: Osso-placa, implante, fratura, estudo mecânico.

INTRODUCTION

Radius and ulna fractures are common in dogs, mainly of the middle and distal thirds of the bone (Phillips 1979, Denny & Butterworth 2000). The distal third fractures are often the most problematic, due to the high incidence of delayed union and nonunion (Sumner-Smith & Cawley 1970, Welch et al. 1997, Denny & Butterworth 2000, Boudrieau 2003). Any of several methods can be employed to immobilize a radial fracture, such as splints or casts, linear or circular external skeletal fixation, and bone plates (Harasen 2003, Milovancev & Ralphs 2004, Probst 2014). Splints or casts

[1] Received on June 7, 2016.

Accepted for publication on July 28, 2016.

[2] Department of Veterinary Surgery and Anesthesiology, School of Veterinary Medicine and Animal Science, Univesidade Estadual Paulista (Unesp), Cx. Postal 560, Rubião Júnior s/n, Botucatu, SP 18618-000, Brazil. *Corresponding author: sheilacr@fmvz.unesp.br

[3] Laboratório de Ensaios Mecânicos e Metalográficos (LEMM), IPAC, Rua Luiz Pengo 145, Jardim Orlando Chesini Neto, Jaú, SP 17212-811, Brazil.

are not recommended for distal third fractures because of the high frequency of complications (Denny & Butterworth 2000, Milovancev & Ralphs 2004). Under these conditions, the fractures are subjected to shear forces that increase the probability of non-union[3]. The linear fixators can be employed, but the use of two pins in the distal segment can be hampered by the short length of the bone (Denny & Butterworth 2000, Piermattei et al. 2006, McCartney et al. 2010). Other options are the hybrid or circular external skeletal fixators that allow a stable fixator configuration by utilizing at least one ring in the distal bone segment (Fox 2012).

Bone plates are the preferred method for the treatment of distal radius fractures since they restore bone stability and allow for early weight bearing (Stifler 2004, Johnson 2013, Probst 2014). Among the implant models and application access routes are: (1) A T-plate applied cranially that allows the use of two or three screws in the short distal bone fragment; (2) Hooked plate that employs two hooks and one screw in the distal bone; (3) Straight plate applied medially that does not interfere with extensor tendons and it incorporates a greater amount of the bone; (4) Straight plate applied cranially. However, these types are dependent on the length of the distal bone fragment (Bellah 1987, Sardinas & Montavon 1997, Balfour et al. 2000, Denny & Butterworth 2000, Hamilton & Hobbs 2005, Piermattei et al. 2006, Haaland et al. 2009, Rose et al. 2009, Uhl et al. 2013).

Although the conventional T-plate achieves good results (Hamilton & Hobbs 2005), the current concepts in the principles of fracture management have influenced the development of locking plate systems (Wagner 2003). By locking the screws to the plate ensures angular and axial stability, besides the biological advantages such as better blood-supply preservation and flexible elastic fixation that favors bone callus formation (Wagner 2003, Miller & Goswami 2007). However, several factors can influence the mechanical behavior of the bone-plate constructs (Miller & Goswami 2007).

Therefore, the present study aimed to develop a locking T-plate designed with locked screw holes and one dynamic compression hole especially intended to be used for distal radial fractures, and to evaluate mechanical properties of bone-plate constructs by using synthetic models.

MATERIALS AND METHODS

Ethics statement. This study followed the guidelines for the care and use of laboratory animals and was approved by the Ethics Committee of our Veterinary School.

Study design. To develop bone-plate design and screws a computerized tomography (Shimadzu SCT-7800CT) was performed on the radius of a Maltese dog (Fig.1). The scanning parameters were 120kVp, 160 mA, 1.0 mm slice thickness, pitch of 1.0, and 1 s/rotation. The images were reconstructed with MPR using Voxer 3D 6.3 (Barco).

Forty T-shaped polyurethane blocks (Synthetic Bone, Nacional Ossos; Jaú, Brazil) (total length = 40 mm, width of proximal portion = 15mm, width of distal portion = 20mm; cortical thickness = 1.0mm [40 pcf Density]; cancellous thickness = 15 mm [40 pcf Density]), and 20 titanium T-plates were used for mechanical testing.

Preparation of bone-plate constructs. Each pair of polyurethane blocks was fixed in a bench vise to simulate a 2mm fracture gap for which bone-plate constructs were assembled. The bone plate was positioned over the polyurethane blocks with the fracture gap between the head and shaft of the plate (Fig.2). The locked holes were drilled with a 2.0–mm drill bit using a specific drill guide (2.7 mm). Holes were drilled first in the head holes of the T-plate, into which two locked self-tapping 2.7mm cortical screws, 12mm long, were placed. The dynamic compression hole was drilled using a neutral drill-guide with a 2.0mm drill bit and filled with a self-tapping 2.7mm cortical screw, 10 mm long. Next holes were drilled in the shaft holes of the T-plate into which the three locked self-tapping 2.7mm cortical screws, 10mm long, were placed. All screws were inserted and tightened with a torque wrench (Torque wrench model TRNA 20PA, Tork Ferramentas Ltda., São Leopoldo, Brazil) by the same investigator. The final insertional torque was 1 Nm for both locked and standard cortical screws.

Mechanical testing. The laboratory and testing machines are according to ISO 17025: 2005. For static testing, six bone-plate constructs were tested to failure, three in axial compression (Fig.3) and three in cantilever bending (Fig.4). These values determined the loads for fatigue testing. The tests were realized using a universal testing machine (Universal testing machine EMIC® DL-10000; São José dos Pinhais, Brazil), with maximum load capacity of 10000 N, supplied with the software (Commercial software TESC for EMIC version 3.04; São José dos Pinhais, Brazil). The endpoint test was determined by contacting of polyurethane blocks and fracture gap closure. For the axial compression test were used two supports with loading rollers. The distance between rollers was of 93mm. A load cell capacity of 10000N with load rate of 3 mm/min was used. In the cantilever bending test the load cell was positioned next to the T-plate head with a lever arm to calculate a bending moment of 45mm. A load cell capacity of 10000N with load rate of 10mm/min was used.

For fatigue testing, 14 bone-plate constructs were tested, seven in axial compression and seven in cantilever bending. Fatigue failure was defined as polyurethane block breakage, or pullout of

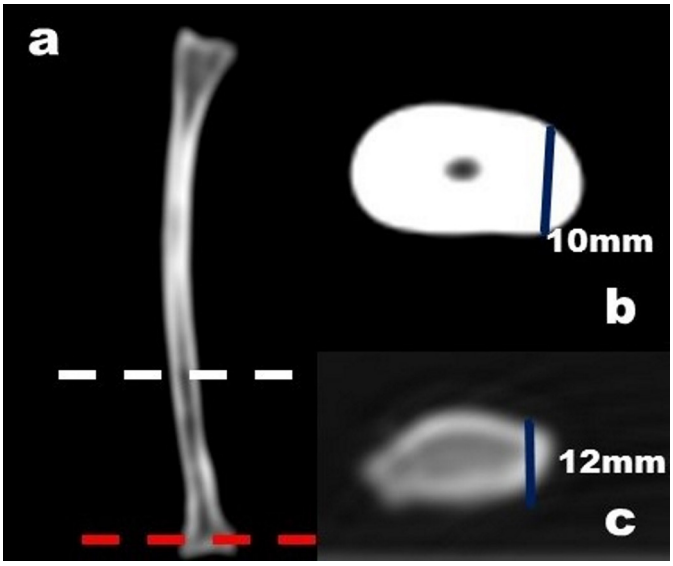

Fig.1. (**a**) Computerized tomography image of the radius of a Maltese dog. (**b**) White and red dashed lines correspond to the regions shown in the images (craniocaudal measurement of the radius diaphyseal) and (**c**) (craniocaudal measurement of distal radius epiphysis), respectively.

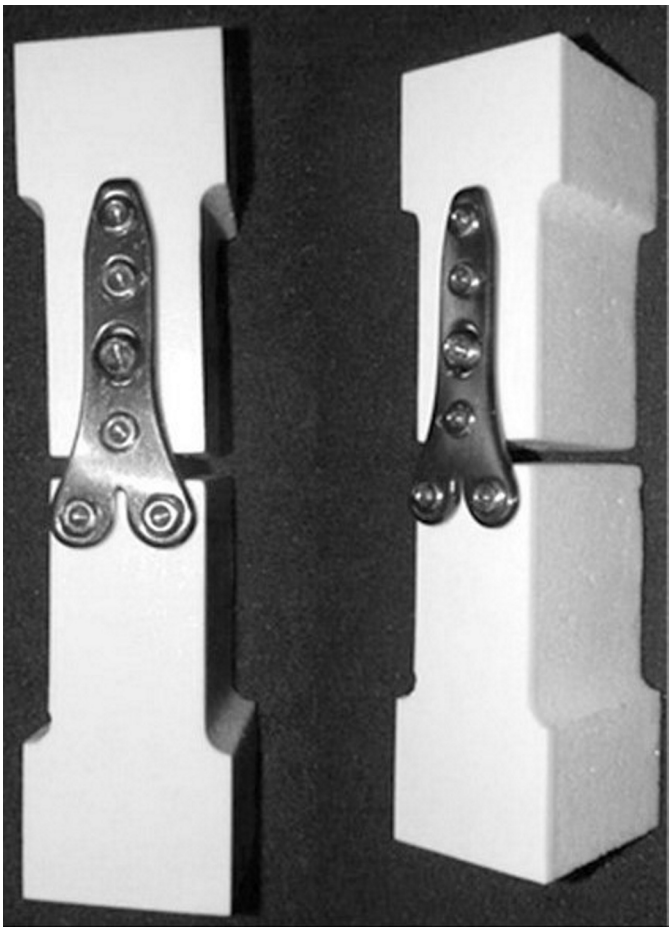

Fig.2. 2.7mm locking T-plate positioned over the polyurethane blocks with the fracture gap between the head and shaft of the plate.

the screws from the polyurethane block, or plate breakage. Tests were discontinued after one million cycles (run-out limit) if the construct had not already failed. All tests were realized at room temperature of approximately 21ºC. Fatigue axial compression tests were carried out by means of a testing machine (MFE 800 LEMM-007 testing machine, Laboratório de Ensaios Mecânicos e Metalográficos; Jaú, Brazil) with 10000N capacity and load cell of 1000 N. Cyclical loads were applied under a controlled load with load ratio of 0.1, reference load of 99.5 N, and frequency of 5 Hz. Fatigue cantilever bending tests were achieved using a testing machine (Brasvalvulas BME2000 160UFI LEMM003, Brasvalvulas Comércio e Serviços Ltda., São Paulo, Brazil) with 20000 N capacity and load cell of 1000 N. Cyclical loads were applied under a controlled load with load ratio of 0.1, reference load of 31.67 N, and frequency of 5 Hz.

Radiographic evaluation. All constructs were radiographed before the mechanical testing, in lateral and craniocaudal positions, to ensure the correct implant placement and discard abnormalities in the polyurethane blocks. After mechanical testing, radiograph exams were performed to detect abnormalities in the polyurethane blocks due to the testing.

RESULTS

Design of the plate

A six-hole 2.7 mm T-plate (Locking T-plate, Biomecânica Indústria e Comércio de Produtos Ortopédicos Ltda.; Jaú, Brazil) (35 mm long and 1.0 mm thick) was developed (Fig. 5). The shaft had a width of 7.0 mm and a length of 30 mm, and three locked screw holes and one dynamic compression hole. The head was 14.2 mm wide and 5 mm long and contained two locked screw holes. The head of the plate had an indentation and the shaft end was tapered-shaped. The head of the cortex bone screws had conventional hexagonal drive. The 2.7 locked screws had 12 mm length (head of the plate) and 10 mm length (shaft of the plate), and the 2.7 unlocked screw had 10 mm length. All screws were self-tapping screws. The plate and screws were composed of titanium alloy (Ti6Al4V – titanium base, 6 aluminum, 4 vanadium) and anodic coating that presents blue coloration.

Radiographic evaluation and mechanical testing

Radiographic evaluation of the constructs did not show any abnormality prior to mechanical testing. The results of the constructs at the static-testing endpoint in axial compression and cantilever bending are displayed in Tables 1 and 2, respectively. In static testing higher values of axial compression test than cantilever bending test were observed for all variables. The results of axial compression and

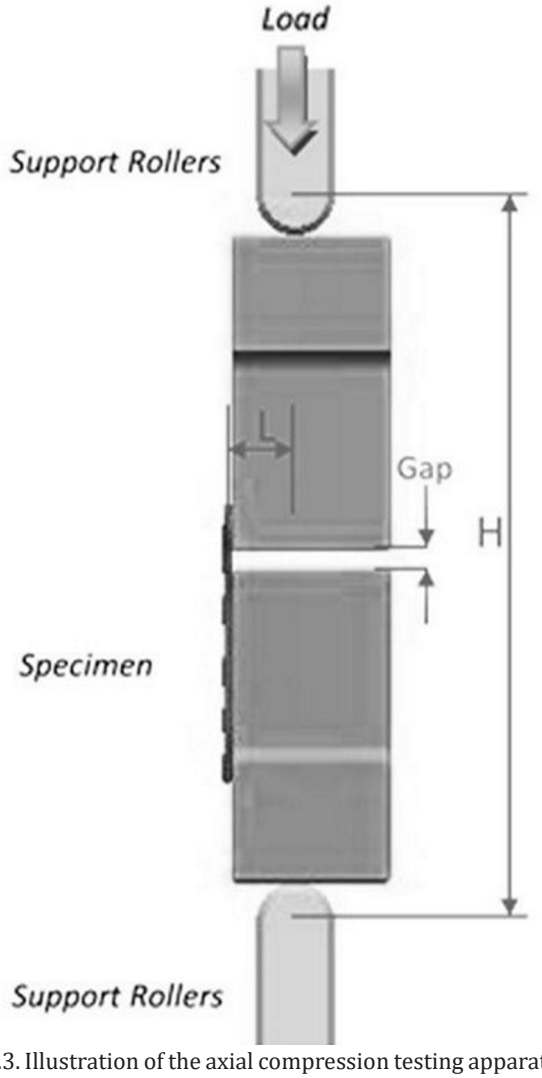

Fig.3. Illustration of the axial compression testing apparatus using two supports with loading rollers.

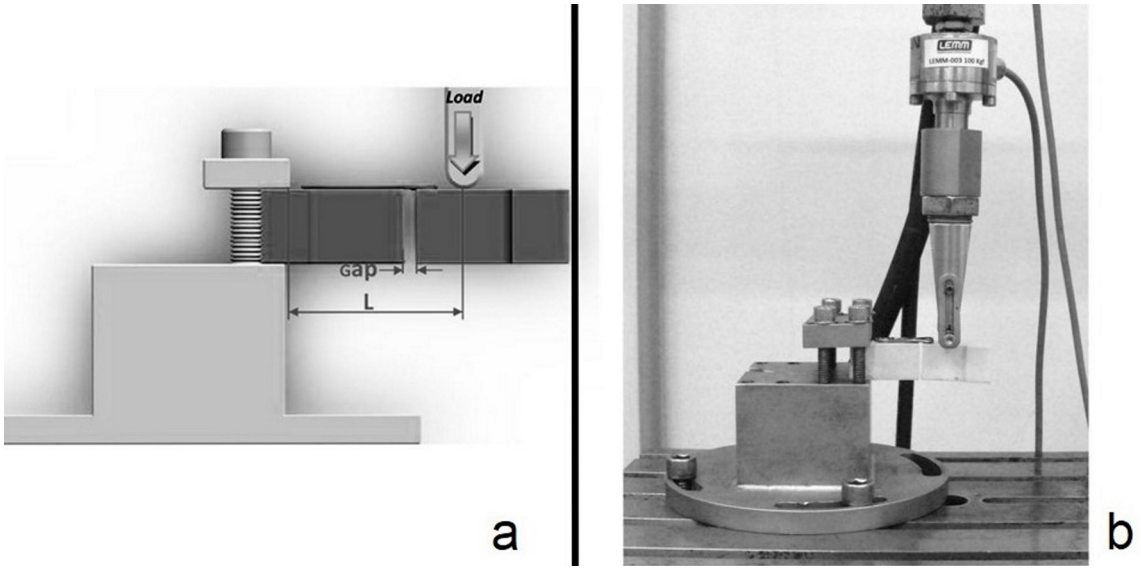

Fig.4. The test setting of a 2,7mm locking T-plate: (**a**,**b**) Illustration and apparatus for cantilever bending testing.

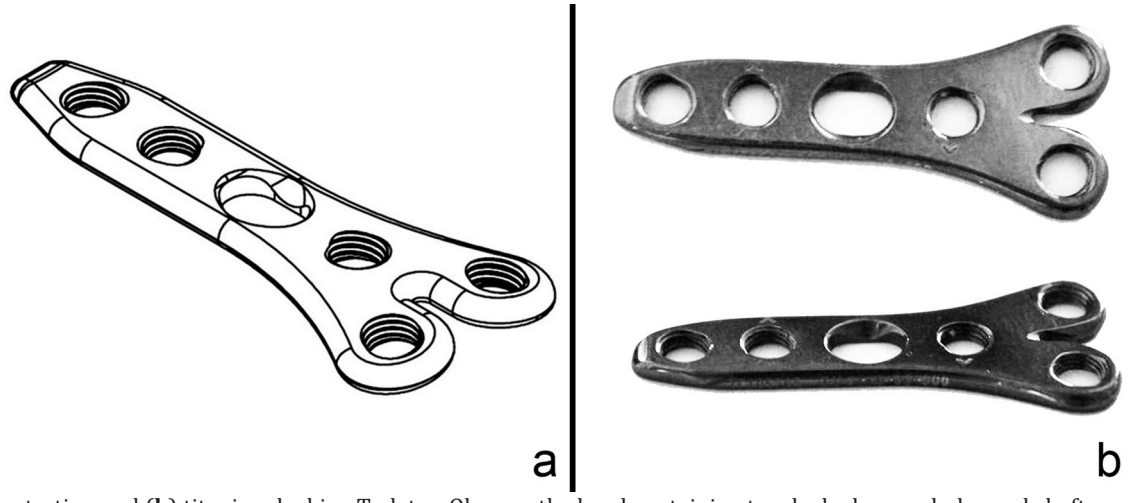

Fig.5. (**a**) Illustration and (**b**) titanium locking T-plates. Observe the head containing two locked screw holes and shaft containing three locked screw holes and one dynamic compression hole.

Table 1. Maximum load and Moment at maximum load obtained in locking T-plate under axial compression static testing

Samples	Maximum load (N)	Moment at maximum load (Nm))
1	100.0	0.80
2	104.0	0.83
3	94.4	0.76
Mean ± SD	99.5 ± 4.8	0.8 ± 0.03
U(%)	0.25	0.25

U = is the estimate of the measurement error due to machine and the error of the load cell. SD = Standard deviation.

Table 2 Maximum load and Moment at maximum load obtained in locking T-plate under cantilever bending static testing

Samples	Maximum load (N)	Moment at maximum load (Nm))
1	30	1.35
2	32	2.02
3	33	1.57
Mean ± SD	31.7 ± 1.5	1.6 ± 0.3
U(%)	0.29	0.29

U = is the estimate of the measurement error due to machine and the error of the load cell. SD = Standard deviation.

cantilever bending fatigue testing are displayed in Tables 3 and 4, respectively. In axial compression fatigue testing all bone-plate constructs withstood 1,000,000 cycles. However, 71% of the constructs showed at the end of the test en bloc pullout of the locked screws in the synthetic bone, two in screws positioned in proximal extremity of the shaft and three in screws positioned in both the proximal shaft extremity and the T-plate head. In cantilever bending fatigue testing, failure occurred before 1,000,000 cycles in four bone-plate constructs. Failures occurred in 57% of the bone-plate constructs because of breaking of the polyurethane block at the screw area (proximal extremity of the plate shaft), of which two were observed in radiographic exams only. Three constructs in fatigue testing did not fail, but one construct showed at the end of the test en bloc pullout of the locked screws in the synthetic bone.

Table 3. Variables evaluated in locking T-plate constructs under axial compression fatigue testing

Constructs	Maximum load (Kgf)	Maximum compression load (N)	Minimum compression load (N)	Maximum moment (Nm)	Minimum moment (Nm))	Number of cycles to failure
1	7.66	75.12	9.02	0.60	0.07	1.003.016
2	11.56	113.36	13.14	0.91	0.11	1.003.016
3	20.65	202.51	21.87	1.62	0.17	1.003.016
4	3.26	31.97	4.51	0.26	0.04	1.003.016
5	4.15	40.70	4.51	0.33	0.04	1.003.016
6	3.28	32.17	3.73	0.26	0.03	1.003.016
7	4.42	43.35	4.51	0.35	0.04	1.003.016

Table 4. Variables evaluated in locking T-plate constructs under cantilever bending fatigue testing

Constructs	Maximum load (Kgf)	Maximum bending load (N)	Minimum bending load (N)	Maximum moment (Nm)	Minimum moment (Nm)	Number of cycles to failure
1	3.44	33.73	4.12	1.52	0.19	1.003.016
2	6.58	64.53	7.55	2.90	0.34	18.826
3	4.98	48.84	5.30	2.20	0.24	54.660
4	3.70	36.28	4.71	1.63	0.21	352.134
5	3.19	31.28	4.90	1.41	0.22	1.003.016
6	3.62	35.50	4.51	1.60	0.20	157.495
7	3.96	38.83	3.63	1.75	0.16	1.003.016

DISCUSSION

The locked T-plate used in the present study presents some details that may improve mechanical efficiency and adjustment of the plate to the underlying bone. The tapered-shaped end of the T-plate shaft facilitates insertion and sliding under soft tissue, whereas an indentation allows adjustment in the distal radius, features that resemble other plate models (Ruchelsman et al. 2010).

The advent of the locking systems has given rise to the development of new bone-plate designs for treating a distal radius fracture in human patients; these include implants with combi holes that allow insertion of locking or standard screws at the same hole, plates containing only locking screw holes, and those with separated locking and non-locking screw holes (Osada et al. 2003, Koh et al. 2006, Willis et al. 2006). The plate used in the present study has a shaft with three locked screw holes used to stabilize the construct and one dynamic compression hole that enables interfragmentary compression.

The biomechanical studies of plating systems in the treatment of distal radial fractures in human medicine have employed a wedge osteotomy model and/or segmental bone gap model (Osada et al. 2004, Koh et al. 2006, Willis et al. 2006). In veterinary medicine, transverse osteotomy was performed to evaluate three methods of plate fixation in distal fracture of the radius (Wallace et al. 1992), and 2 mm gap to analyze stacked plating techniques to stabilize distal radial fractures (Rose et al. 2009). The present study also employed a 2 mm segmental gap in order to simulate an unstable extra-articular fracture of the distal radius. Moreover, in a study using human cadaver radii, the segmental resection osteotomy model was not significantly stiffer than the wedge model, but the latter model failed under a higher load (Koh et al. 2006).

In the present study, we chose synthetic specimens due to difficulty in procuring similar samples of canine radii as well as obtaining ethics approval to use cadavers. Anatomical models of synthetic radius bone would be ideal, but polyurethane blocks having a T-shaped were necessary to achieve better fixation in relation to the testing machines. PVC pipes (outer diameter 22mm; inner diameter 15mm) were used in a study that evaluated veterinary cuttable plates in a fracture model of the distal radius in small breed dogs (Rose et al. 2009). In the current study, the cortical thickness was 1 mm, but due to the cancellous bone height of 15mm, the screws incorporate just one cortex.

Several biomechanical tests have used to evaluate plates for the distal radial fractures in humans, such as axial compression until failure, fatigue axial compression, and cantilever bending (Osada et al. 2003, Osada et al. 2004, Koh et al. 2006, Willis et al. 2006). Veterinary medical research has employed a non-destructive axial loading test followed by testing to failure (Wallace et al. 1992), axial compression fatigue testing (Rose et al. 2009), and load applied axially and cyclically in conditions that allow bending (Uhl et al. 2013).

In the current study, higher values of axial compression test than cantilever bending test were observed for all variables in static testing. In a biomechanical study that compared the stability of five models of distal radial plates for humans was observed higher values of axial compressive stiffness than bending stiffness values for all models (Willis et al. 2006). In the present study the maximum load applied to the constructs in fatigue testing was a percentage of the values obtained in the static testing. In another study, the maximum load was 54N and 90N considered as 100% of the axial load placed on the radius by 5.5 and 9.1 kg dogs (Rose et al. 2009). Therefore, in the present study

the constructs probably are able to support the load of approximately 3-7 kg dogs, in both axial and cantilever bending loading. However, more studies are necessary using the implant *in vivo*.

Cyclic load tests can simulate more realistically the influence of repetitive loads to which the implants are submitted during the postoperative period (Turner & Burr 1993, Cordey 2000, Chao et al. 2013). The performance of the constructs in resisting fatigue in the present study was better in fatigue axial compression test than fatigue cantilever bending. Moreover, the constructs under fatigue axial compression test supported a larger number of cycles prior to failure. The direction and magnitude of the physiological loads on the distal radius in dogs must be considered in biomechanical evaluation. The plate applied to the cranial surface of the radius in general neutralizes the tension forces, when an axial load is applied (Wallace et al. 1992, Boudrieau 2003), a fact that reinforces the validity of the construct evaluated.

Failure modes are dependent on construct characteristics (plate/screw/bone)[34]. Locked plate constructs allow forces to be transferred through a threaded connection between the plate and the screw (Cronier et al. 2010), so the failure occurs due to a monoblock effect with the screws being forced together (Haidukewych 2004, Cronier et al. 2010). At the end of the axial compression fatigue testing in the present study was observed that 71% of the constructs showed pullout of the locked screws, although all constructs had withstood 1,000,000 cycles. The higher pullout force acting in these screws must be considered in cases that reduce the screw numbers to produce more flexible bone-plate construct. On the other hand, in cantilever bending fatigue 57% of the construct failures were due to breaking of the polyurethane blocks.

This study has limitations, the first of which being the nonuse of a synthetic model that simulates the shape of the canine bone. Another limitation relates to the number of screws that must be evaluated in further studies. Finally, comparisons between different models of plates might have provided more information.

CONCLUSION

The locking T-plate designed with locked screw holes and one dynamic compression hole has mechanical properties that offer greatest resistance to fracture under axial loading than bending forces.

Acknowledgements.- The authors are grateful to the Capes and CNPq.

Conflict of interest statement.- The authors have no competing interests.

REFERENCES

Balfour R.J., Boudrieau R.J. & Gores B.R. 2000. T-Plate fixation of distal radial closing wedge osteotomies for treatment of angular limb deformities in 18 dogs. Vet. Surg. 29:207-217.

Bellah J.R. 1987. Use of a double hook plate for treatment of a distal radial fracture in a dog. Vet. Surg. 16:278-282.

Boudrieau R.J. 2003. Fractures of the radius and ulna, p.1953-1973. In: Slatter D. (Ed.), Textbook of Small Animal Surgery. 3rd ed. W.B. Saunders, Philadelphia.

Chao P., Conrad B.P., Lewis D.D., Horodyski M. & Pozzi A. 2013. Effect of plate working length on plate stiffness and cyclic fatigue life in cadaveric femoral fracture gap model stabilized with a 12-hole 2.4mm locking compression plate. BMC Vet. Res. 9:1-7.

Cordey J. 2000. Introduction: basic concepts and definitions in mechanics. Injury 1:B1-B13.

Cronier P., Pietu G., Dujardin C., Bigorre N., Ducellier F. & Gerard R. 2010. The concept of locking plates. Orthop. Traumat. Surg. Res. 96:S17-S36.

Denny H.R. & Butterworth S.J. 2000. The radius and ulna, p.389-408. In: Denny H.R. & Butterworth S.J. (Eds), A Guide to Canine and Feline Orthopaedic Surgery. 4th ed. Blackwell Science, UK.

Fox D.B. 2012. Radius and ulna, p.760-784. In: Tobias K.M. & Johnston S.A. (Eds), Veterinary Surgery: small animal. Elsevier Saunders, St Louis.

Haaland P.J., Sjöström L., Devor M. & Haug A.A. 2009. Appendicular fracture repair in dogs using the locking compression plate system: 47 cases. Vet. Comp. Orthop. Traumatol. 22:309-315.

Haidukewych G.J. 2004. Innovations in Locking Plate Technology. J. Am. Orthop. Surg. 12:205-212.

Hamilton M.H. & Hobbs S.J.L. 2005. Use of the AO veterinary mini 'T'-plate for stabilisation of distal radius and ulna fractures in toy breed dogs. Vet. Comp. Orthop. Traumatol. 18:18-25.

Harasen G. 2003. Common long bone fracture in small animal practice. Part 2. Can. Vet. J. 44:503-504.

Johnson A.L. 2013. Fundamentals of orthopedic surgery and fracture management, p.1033-1105. In: Fossum T.W. (Ed.), Small Animal Surgery. 4th ed. Elsevier Mosby, St Louis.

Koh S., Morris R.P., Patterson R.M., Kearney J.P., Buford W.L. & Viegas S.F. 2006. Volar fixation for dorsally angulated extra-articular fractures of the distal radius: a biomechanical study. J. Hand Surg. Am. 31:771-779.

McCartney W., Kiss K. & Robertson I. 2010. Treatment of distal radial/ulnar fractures in 17 toy breed dogs. Vet. Rec. 166:430-432.

Miller D.L. & Goswami T. 2007. A review of locking compression plate biomechanics and their advantages as internal fixators in fracture healing. Clin. Biomech. 22:1049-1062.

Milovancev M. & Ralphs S.C. 2004. Radius/ulna fracture repair. Clin. Tech. Sm. Anim. Pract. 19:128-133.

Osada D., Viegas S.F., Shah M.A., Morris R.P. & Patterson R.M. 2003. Comparison of different distal radius dorsal and volar fracture fixation plates: A biomechanical study. J. Hand Surg. Am. 28:94-104.

Osada D., Fujita S., Tamai K., Iwamoto A., Tomizawa K. & Saotome K. 2004. Biomechanics in uniaxial compression of three distal radius volar plates. J. Hand Surg. Am. 29:446–451.

Phillips I.R. 1979. A survey of bone fractures in the dog and cat. J. Small Anim. Pract. 20:661-674.

Piermattei D.L., Flo G.L. & De Camp C.E. 2006. Fractures of the radius and ulna, p.359-381. In: Piermattei D.L., Flo G.L. & De Camp C.E. (Eds), Brinker, Piermattei, and Flo's Handbook of Small Animal Orthopedics and Fracture Repair. 4th ed. W.B. Saunders, Philadelphia.

Probst C.W. 2014. Repairs of fractures of the radius and ulna, p.933-942. In: Bojrab M.J. (Ed.), Current Techniques in Small Animal Surgery. 5th ed. Taylor and Francis Group, Philadelphia.

Rose B.W., Pluhar G.E., Novo R.E. & Lunos S. 2009. Biomechanical analysis of stacked plating techniques to stabilize distal radial fractures in small dogs. Vet. Surg. 38:954-960.

Ruchelsman D.E., Mudgal C.S. & Jupiter J.B. 2010. The role of locking technology in the hand. Hand Clin. 26:307-319.

Sardinas J.C. & Montavon P.M. 1997. Use of a medial bone plate for repair of radius and ulna fractures in dogs and cats: a report of 22 cases. Vet. Surg. 26:108-113.

Stifler K.S. 2004. Internal fracture fixation. Clin. Tech. Small Anim. Pract. 19:105-113.

Sumner-Smith G. & Cawley A.J. 1970. Nonunion of fractures in the dog. J. Sm. Anim. Pract. 11:311-325.

Turner C.H. & Burr D.B. 1993. Basic biomechanical measurements of bone: a tutorial. Bone. 14:595-608.

Uhl J.M., Kapatkin A.S., Garcia T.C. & Stover S.M. 2013. *Ex vivo* biomechanical comparison of a 3.5 mm locking compression plate applied cranially and a 2.7mm locking compression plate applied medially in a gap model of the distal aspect of the canine radius. Vet. Surg. 42:840-846.

Wagner M. 2003. General principles for the clinical use of the LCP. Injury 34:S-B31-42.

Wallace M.K., Boudrieau R.J., Hyodo K. & Torzilli P.A. 1992. Mechanical evaluation of three methods of plating distal radial osteotomies. Vet. Surg. 21:99-106.

Welch J.A., Boudrieau R.J., Dejardin L.M. & Spodnick G.J. 1997. The intraosseous blood supply of the canine radius: implications for healing of distal fractures in small dogs. Vet. Surg. 26:57-61.

Willis A.A., Kutsumi K., Zobitz M.E. & Cooney III W.P. 2006. Internal fixation of dorsally displaced fractures of the distal part of the radius. J. Bone Joint Surg. 88A:2411-2417.